Received: 7 April 2018 | Revised: 7 May 2018 | Accepted: 15 May 2018

DOI: 10.1111/odi.12900

ORIGINAL ARTICLE

WILEY ORAL DISEASES

Abnormal bone remodelling activity of dental follicle cells from a cleidocranial dysplasia patient

Yang Liu[1] | Xianli Zhang[1,2] | Xiangyu Sun[1] | Xiaozhe Wang[1] | Chenying Zhang[1] | Shuguo Zheng[1]

[1]Department of Preventive Dentistry, Peking University School and Hospital of Stomatology, National Engineering Laboratory for Digital and Material Technology of Stomatology, Beijing Key Laboratory of Digital Stomatology, Beijing, China

[2]Department of Stomatology, Xuanwu Hospital Capital Medical University, Beijing, China

Correspondence
Shuguo Zheng and Chenying Zhang, Department of Preventive Dentistry, Peking University School and Hospital of Stomatology, 22 Zhongguancun Avenue South, Haidian District, Beijing 100081, PR China.
Emails: zhengsg86@gmail.com; zhengchy168@163.com

Funding information
National Natural Science Foundation of China, Grant/Award Number: 81771053; Peking University School and Hospital of Stomatology Science Foundation for Young Scientists, Grant/Award Number: PKUSS20160105

Abstract

Objectives: To explore the role of dental follicle cells (DFCs) with a novel cleidocranial dysplasia (CCD) causative gene *RUNX2* mutation ($DFCs^{RUNX2+/m}$) in delayed permanent tooth eruption.

Materials and methods: A CCD patient with typical clinical features was involved in this study. $DFCs^{RUNX2+/m}$ were cultured and DNA was extracted for *RUNX2* mutation screening. Measurements of cell proliferation, alkaline phosphatase (ALP) activity, alizarin red staining and osteoblast-specific genes expression were performed to assess osteogenesis of $DFCs^{RUNX2+/m}$. Co-culture of DFCs and peripheral blood mononuclear cells (PBMCs), followed tartrate-resistant acid phosphatase (TRAP) staining, real-time PCR and western blot were performed to evaluate osteoclast-inductive capacity of $DFCs^{RUNX2+/m}$.

Results: A missense *RUNX2* mutation (c. 557G>C) was found in $DFCs^{RUNX2+/m}$ from the CCD patient. Compared with normal controls, this mutation did not affect the proliferation of $DFCs^{RUNX2+/m}$, but down-regulated the expression of osteogenesis-related genes, leading to a decrease in ALP activity and mineralisation. Co-culture results showed that $DFCs^{RUNX2+/m}$ reduced the formation of $TRAP^{+}$ multinucleated cells and the expression of osteoclastogenesis-associated genes. Furthermore, the mutation reduced the ratio of RANKL/OPG in $DFCs^{RUNX2+/m}$.

Conclusions: $DFCs^{RUNX2+/m}$ disturbs bone remodelling activity during tooth eruption through RANK/RANKL/OPG signalling pathway and may thus be responsible for impaired permanent tooth eruption in CCD patients.

KEYWORDS

cleidocranial dysplasia, delayed tooth eruption, dental follicle cells, osteoclastogenesis, osteogenesis, *RUNX2* mutation

1 | INTRODUCTION

Cleidocranial dysplasia (CCD; MIM 119600) is a rare generalised dysplasia of osseous and dental tissues with incidence estimated at 1:1,000,000 (Mundlos et al., 1997). The main clinical manifestation includes absence or hypoplasia of clavicle, delayed closing of fontanelle, short stature and multiple dental anomalies such as retention of primary teeth, impaction of permanent teeth, and supernumerary teeth (Mundlos, 1999). CCD exhibits autosomal dominant heredity with complete penetrance, while the phenotypic spectrum of CCD individuals varies dramatically (Quack et al., 1999).

According to previous studies, mutation of the runt-related transcription factor-2 (*RUNX2*) gene was closely associated with the patients who were diagnosed with CCD according to the clinical

manifestation (Yoshida et al., 2002). As a crucial transcription factor, RUNX2 plays an important role in bone metabolism by regulating osteoblasts and osteoclasts differentiation. In vitro and in vivo study had proved that RUNX2 is critical for both endochondral and intramembranous ossification, and RUNX2 plays essential roles in regulating the expression of osteogenesis-specific genes (Bruderer, Richards, Alini, & Stoddart, 2014). RUNX2 can also regulate the secretion of receptor activator of nuclear factor kappa B ligand (RANKL) and osteoprotegerin (OPG) in osteoblasts and then indirectly regulates osteoclastogenesis through RANK/RANKL/OPG signalling pathway (Enomoto et al., 2003; Li et al., 2014). In addition, RUNX2 binding sites have been found in the promoter region of RANKL and OPG, illustrating that RUNX2 can directly regulate the expression of RANKL and OPG (Byon et al., 2011; Thirunavukkarasu et al., 2001).

Despite the numerous skeletal deficiencies observed in CCD individuals, the dental anomalies are usually their main complaints, especially for impaired permanent tooth eruption (Jensen & Kreiborg, 1990). During the stage of tooth eruption, alveolar bone remodelling is tightly orchestrated by dental follicle, a loose ecto-mesenchymal tissue that surrounds the developing tooth germ, in a spatiotemporal manner (Wise, 2009; Wise & King, 2008). Dental follicles are able to produce molecules such as colony-stimulating factor-1 (CSF-1), monocyte chemotactic protein-1 (MCP-1) and RANKL at certain times to promote osteoclastogenesis and increase alveolar bone resorption for the establishment of tooth eruption pathway (Liu, Yao, Pan, & Wise, 2005; Que & Wise, 1997; Yao, Ring, Henk, & Wise, 2004). In addition, dental follicle cells (DFCs) are precursors of alveolar osteoblasts and have been reported to participate in the procedure of alveolar bone formation, which probably functions as a motive force for tooth eruption (Pan et al., 2010; Saugspier et al., 2010; Wise, He, Gutierrez, Ring, & Yao, 2011; Wise, Yao, & Henk, 2007). Thus, DFCs participate in tooth eruption not only as a regulator of bone activity but also as the precursors of alveolar osteoblasts, which are critical for bone formation during tooth eruption.

RUNX2 had been reported to be expressed in dental epithelium, dental papilla and dental follicles during tooth development and eruption (Camilleri & McDonald, 2006). In addition, *RUNX2* mutations would produce negative effects on expression of the RUNX2 protein in DFCs and periodontal ligament cells (PDLCs) of CCD patients (Chen et al., 2014; Li et al., 2014; Yoda, Suda, Kitahara, Komori, & Ohyama, 2004). However, the regulatory mechanism responsible for the delayed permanent tooth eruption mediated by DFCs in CCD patients has not been completely understood yet. In this study, we hypothesised that the *RUNX2* mutation found in the CCD patient might interfere with the bone remodelling function of DFCs. To verify this hypothesis, primary DFCs were collected from one CCD patient ($DFCs^{RUNX2+/m}$) and normal controls ($DFCs^{RUNX2+/+}$), and the effects of $DFCs^{RUNX2+/m}$ on osteogenesis and osteoclastogenesis were explored.

2 | MATERIALS AND METHODS

2.1 | Participants

A 43-year-old woman, diagnosed with CCD according to clinical findings, and three unaffected women (aged 40–45 years) participated in the present research with understanding and written consent. This study was approved by the Ethical Committee of Peking University School of Stomatology (IRB-2012004). All the methods were carried out according to the relevant guidelines and the Declaration of Helsinki.

2.2 | Cell culture

Dental follicle tissues were gathered during surgical treatment of impacted maxillary incisors. To get single DFCs suspension, dental follicles were digested in 0.3% collagenase type I (Sigma-Aldrich, MO, USA) for 40 min at 37°C. Then, the cells were cultured in a growth medium containing DMEM (Gibco, NY, USA), 10% foetal bovine serum (Gibco), 100 U/mL penicillin and streptomycin (Gibco) in an incubator at 37°C with 5% CO_2. The DFCs between 3 and 5 passages were used in subsequent experiments.

2.3 | Mutation analysis

To detect *RUNX2* status in DFCs from the CCD patient and normal controls, we extracted DNA from DFCs with a General AllGen Kit (Cwbiotech, Beijing, China) according to manufacture's protocol. Exon 2 of *RUNX2* gene was amplified by polymerase chain reaction (PCR), and the PCR products were then sequenced with an ABI 3730 sequencer.

2.4 | Immunohistochemistry

For immunohistochemistry staining, DFCs seeded on coverslips were fixed in 4% paraformaldehyde (Sigma-Aldrich) for 20 min, permeated with 0.3% Triton X-100 (Sigma-Aldrich) for 10 min, blocked in bovine serum, and incubated with primary antibodies against cytokeratin and vimentin (Zhongshan Bioengineering, Beijing, China) overnight at 4°C. The SP immunohistochemistry kit and a 3, 3′-diaminobenzidine colouration kit (Zhongshan Bioengineering) were used for the followed staining procedure according to the protocol of the manufacturer. The results were observed and collected by a light microscope equipped with a camera (Carl Zeiss, TH, Germany).

2.5 | Cell proliferation assay

Dental follicle cells were seeded in 96-well plates at the cell density of 2×10^3 cells/well. After incubation for 4 hours, the Cell Counting Kit 8 (CCK-8, Dojindo, Kumamoto, Japan) was used according to

manufacture's instruction. The optical density at 450 nm was examined using a microplate reader (BioTek, VT, USA) every 24 hr for 14 days after seeding.

2.6 | ALP activity test, ALP staining and alizarin red staining

For osteogenic induction, DFCs were seeded at a density of 1×10^5 cells/well in 6-well plates. When 80% confluence was reached, the medium was changed to the osteogenic induction medium (OIM) containing 50 μg/ml ascorbic acid, 10 mM/L β-glycerophosphate, and 100 nM/L dexamethasone (Sigma-Aldrich). After osteogenic induction for 7 and 14 days, alkaline phosphatase (ALP) activity was carried out using an ALP assay kit (Nanjing Jiancheng Bioengineering Institute, Nanjing, China) according to manufacture's protocol. ALP staining was analysed by the NBT/BCIP staining kit (Cwbiotech, Beijing, China) after culturing in OIM for 14 days. For Alizarin red staining, after induction for 21 days in OIM, DFCs were fixed with 95% ethanol for 20 min and incubated with 2% alizarin red for 20 min at room temperature. The image of ALP staining and alizarin red staining were captured by a scanner (HP, CA, USA).

2.7 | Co-culture of DFCs and PBMCs

Co-culture of DFCs and human peripheral blood mononuclear cells (PBMCs) was established for induction of osteoclasts. First, DFCs were plated in 24-well plates at the density of 3×10^4 cells/well. The next day, human peripheral blood was obtained from 2 healthy volunteers, and PBMCs were extracted using Ficoll-paque reagent (GE Healthcare, PA, USA) by density gradient centrifugation. Then the PBMCs were seeded into the same 24-well plate at the density of 3×10^6 cells/well, and 10^{-7} M/L $1\alpha,25\text{-}(OH)_2D_3$ was added to the medium for osteoclasts differentiation.

2.8 | Tartrate-resistant acid phosphatase staining and quantification

After co-cultivation for 14 days, the cells were stained with tartrate-resistant acid phosphatase (TRAP) Kit (Sigma-Aldrich) according to the manufacturer's instructions. The images of TRAP staining were captured by a light microscope, and $TRAP^+$ multinuclear cells were counted as described previously (Wang et al., 2016).

2.9 | Real-time PCR

After DFCs were cultured in OIM for 14 days or co-cultured with PBMCs for 14 days, total RNA was extracted with TRIzol reagent (Invitrogen, CA, USA), and reversely transcribed into cDNA with a reverse transcription kit (Thermo Fisher, MA, USA). Real-time PCR was performed using the SYBR Green PCR kit (Roche Applied Science, IN, USA) on an ABI 7500 Real-time PCR System (Applied Biosystems, CA, USA) and GAPDH was used for normalisation. The primers used in this process are listed in Table 1.

2.10 | Western blotting analysis

After DFCs were cultured in OIM for 14 days or co-cultured with PBMCs for 14 days, the total protein was extracted using the RIPA kit (Huaxing bio, Beijing, China). Protein concentration was measured with a BCA kit (Thermo Fisher). The lysate was electrophoresed in 10% SDS-PAGE gels and transferred to PVDF membranes (Millipore, MA, USA). After being blocked in 5% skim milk, membranes were incubated with primary antibodies against RUNX2 (CST, MA, USA), OSX (Abcam, Cambridge, UK), ALP (Abcam), CTSK (Abcam), CTR (Bio-Rad, CA, USA), GAPDH (CST), and β-actin (CST). All the primary antibodies were used at a dilution of 1:1,000. HRP-conjugated secondary antibodies (Jackson ImmunoResearch, PA, USA) were then used. The immune-reactive bands were visualised by the enhanced chemiluminescence

TABLE 1 Sequences primers of selected genes designed for real-time PCR

Genes	Forward primer	Reverse primer
GAPDH	CGACAGTCAGCCGCATCTT	CCAATACGACCAAATCCGTTG
RUNX2	GATGACACTGCCACCTCTGAC	GGGATGAAATGCTTGGGAAC
ALP	GACCTCCTCGGAAGACACTC	TGAAGGGCTTCTTGTCTGTG
OSX	CCTCCTCAGCTCACCTTCTC	GTTGGGAGCCCAAATAGAAA
OCN	AGCAAAGGTGCAGCCTTTGT	GCGCCTGGGTCTCTTCACT
OPN	ATGATGGCCGAGGTGATAGT	ACCATTCAACTCCTCGCTTT
NFATc1	TGTGCCGGAATCCTGAAACTC	GAGCATTCGATGGGGTTGGAG
CTSK	ACTCAAAGTACCCCTGTCTCAT	CCACAGAGCTAAAAGCCCAAC
CTR	TGAAAACAATCGAACCTGGTCC	AAGAATGACCCACAATAGCCAAA
TRAP	TGAGGACGTATTCTCTGACCG	CACATTGGTCTGTGGGATCTTG
CSF-1	AGACCTCGTGCCAAATTACATT	AGGTGTCTCATAGAAAGTTCGGA
RANKL	CAACATATCGTTGGATCACAGCA	GACAGACTCACTTTATGGGAACC
OPG	CACAAATTGCAGTGTCTTTGGTC	TCTGCGTTTACTTTGGTGCCA

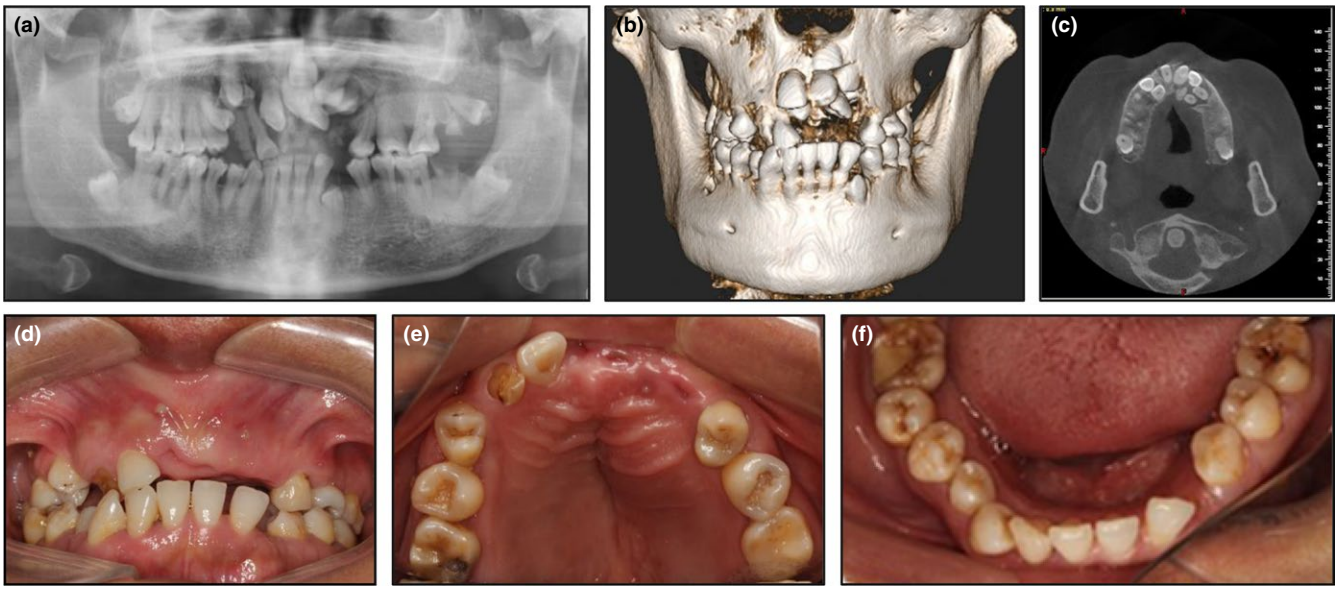

FIGURE 1 Clinical and radiological manifestation of the CCD patient in this study. (a–c) Panoramic radiograph and Cone-beam CT showed retained deciduous teeth, delayed eruption of permanent teeth and supernumerary teeth in the maxillary anterior region. (d–f) The intraoral photograph showed delayed eruption of permanent teeth [Colour figure can be viewed at wileyonlinelibrary.com]

blotting kit (Cwbiotech). The intensities of the bands were quantified using Quantity One software (Bio-Rad, CA, USA). GAPDH or β-actin was used as the internal control.

2.11 | ELISA test

The conditioned medium (CM) of the co-culture system was collected after cultivation for 3 days. Then enzyme-linked immunosorbent assay (ELISA) was performed using commercial kits (Cusabio, Wuhan, China) to measure the concentration of RANKL and OPG in CM. The absorbance at 450 nm was examined by a microplate reader (BioTeK).

2.12 | Statistical analysis

All the experiments were repeated at least 3 times independently. All data were presented as the mean and standard deviation. Student's two-tailed *t*-test was used to compare mean values between groups. $p < 0.05$ was considered statistically significant.

3 | RESULTS

3.1 | Clinical manifestation of the CCD patient

This CCD patient was a sporadic case with typical phenotypes, including hypoplastic clavicles, delayed closure of the anterior fontanelle, concave face type and classic dental abnormalities. The chest radiograph of the patient had been presented in the previous papers of our research group (Zhang et al., 2017). Radiological and clinical examination showed that the right primary maxillary canine was retained, the maxillary permanent anterior teeth were impacted, and 8 supernumerary teeth were present in the alveolar bones (Figure 1a–f).

3.2 | *RUNX2* mutation reduced RUNX2 expression in DFCs while had no effect on the proliferation of DFCs

To identify the mutation of *RUNX2* in the DFCs from the CCD patient, sequencing analysis was performed in the coding region of *RUNX2* gene. As shown in Figure 2a, a missense mutation of *RUNX2* (c. 557G>C, p. R186T) was detected by Sanger sequencing with DNA from the DFCs of the CCD patient, which was consistent with the result using blood samples in our previous study (Zhang et al., 2017). The effect of *RUNX2* mutation on the biological characterisation of DFCs was explored using primary DFCs isolated from the CCD patient ($DFCs^{RUNX2+/m}$) and normal controls ($DFCs^{RUNX2+/+}$). Immunohistochemical staining of vimentin and keratin was carried out to detect the source of the cultured cells. $DFCs^{RUNX2+/m}$ and $DFCs^{RUNX2+/+}$ were vimentin-positive and keratin-negative (Figure 2b), indicating that these cells were derived from mesenchymal cells. Quantitative analysis of cell proliferation by CCK-8 assay showed that the missense *RUNX2* mutation did not affect proliferation rate of $DFCs^{RUNX2+/m}$ ($p > 0.05$) (Figure 2c). The effect of the detected *RUNX2* mutation on RUNX2 expression was then investigated. Real-time PCR and western blot results showed that the mRNA and protein levels of RUNX2 in $DFCs^{RUNX2+/m}$ were significantly lower than $DFCs^{RUNX2+/+}$ ($p < 0.05$) (Figure 2d,e).

3.3 | $DFCs^{RUNX2+/m}$ exhibited weaker osteogenic potential than $DFCs^{RUNX2+/+}$

DFCs are multipotent mesenchymal stem cells that can differentiate into osteoblasts, adipocytes, chondrocytes, and neural cells under

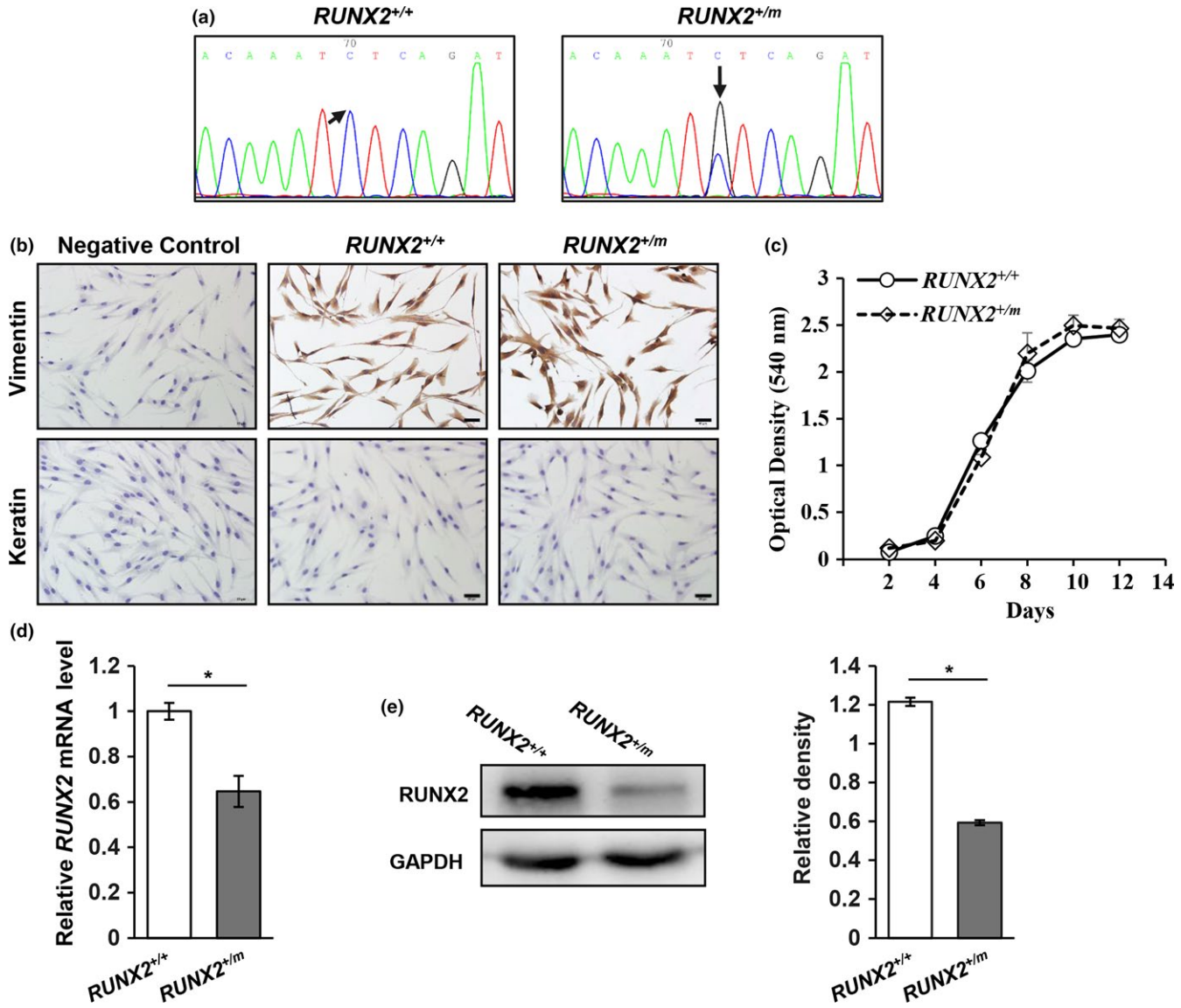

FIGURE 2 *RUNX2* mutation reduced RUNX2 expression while had no effect on the proliferation of DFCs. Primary DFCs were isolated from normal controls (DFCs$^{RUNX2+/+}$) and the cleidocranial dysplasia patient (DFCs$^{RUNX2+/m}$). (a) Reverse sequencing data of *RUNX2* gene from DFCs$^{RUNX2+/+}$ and DFCs$^{RUNX2+/m}$. Arrows indicated the mutation site. (b) Immunohistochemistry staining of vimentin and keratin for DFCs. Scale bar, 50 μm. (c) CCK8 proliferation assay for DFCs at indicated time points. (d) Quantitative analysis of the mRNA level of *RUNX2* in DFCs. (e) Western blotting and quantification of RUNX2 expression in DFCs. *$p < 0.05$ [Colour figure can be viewed at wileyonlinelibrary.com]

different in vitro conditions (Saugspier et al., 2010). In this study, the effect of *RUNX2* mutation on the osteogenic differentiation of DFCs was explored. As ALP is confirmed to be an early marker of mineralisation after osteogenic induction (Zhang et al., 2015), the effect of *RUNX2* mutation on ALP activity of DFCs was first investigated. We found that the ALP activity of DFCs$^{RUNX2+/+}$ increased approximately 1.5-fold after osteogenic induction for 7 days or 14 days ($p < 0.05$) (Figure 3a,b). The ALP activity in DFCs$^{RUNX2+/m}$ was reduced 30%–55% compared with DFCs$^{RUNX2+/+}$ whether under osteogenic induction or not ($p < 0.05$) (Figure 3a,b). ALP staining showed that ALP expression in DFCs$^{RUNX2+/m}$ was lower than that of DFCs$^{RUNX2+/+}$ at basal level, and the difference was much clearer after osteogenic induction (Figure 3c), showing a similar result with ALP activity. Alizarin red staining showed that the mineralised nodules in DFCs$^{RUNX2+/m}$ were obviously fewer than the normal control after osteogenic induction for 21 days (Figure 3d), indicating reduced mineralisation in DFCs$^{RUNX2+/m}$.

Thereafter, the expression of osteoblast-specific genes in DFCs$^{RUNX2+/m}$ and DFCs$^{RUNX2+/+}$ was investigated. Compared with normal controls, the mRNA level of *RUNX2* in DFCs$^{RUNX2+/m}$ was decreased approximately 40% both in basal and osteogenic media ($p < 0.05$) (Figure 3e). Consistently, the mRNA level of osteogenic markers, such as *ALP*, osterix (*OSX*), osteocalcin (*OCN*) and osteopontin (*OPN*), was reduced 20%–50% in DFCs$^{RUNX2+/m}$ whether under

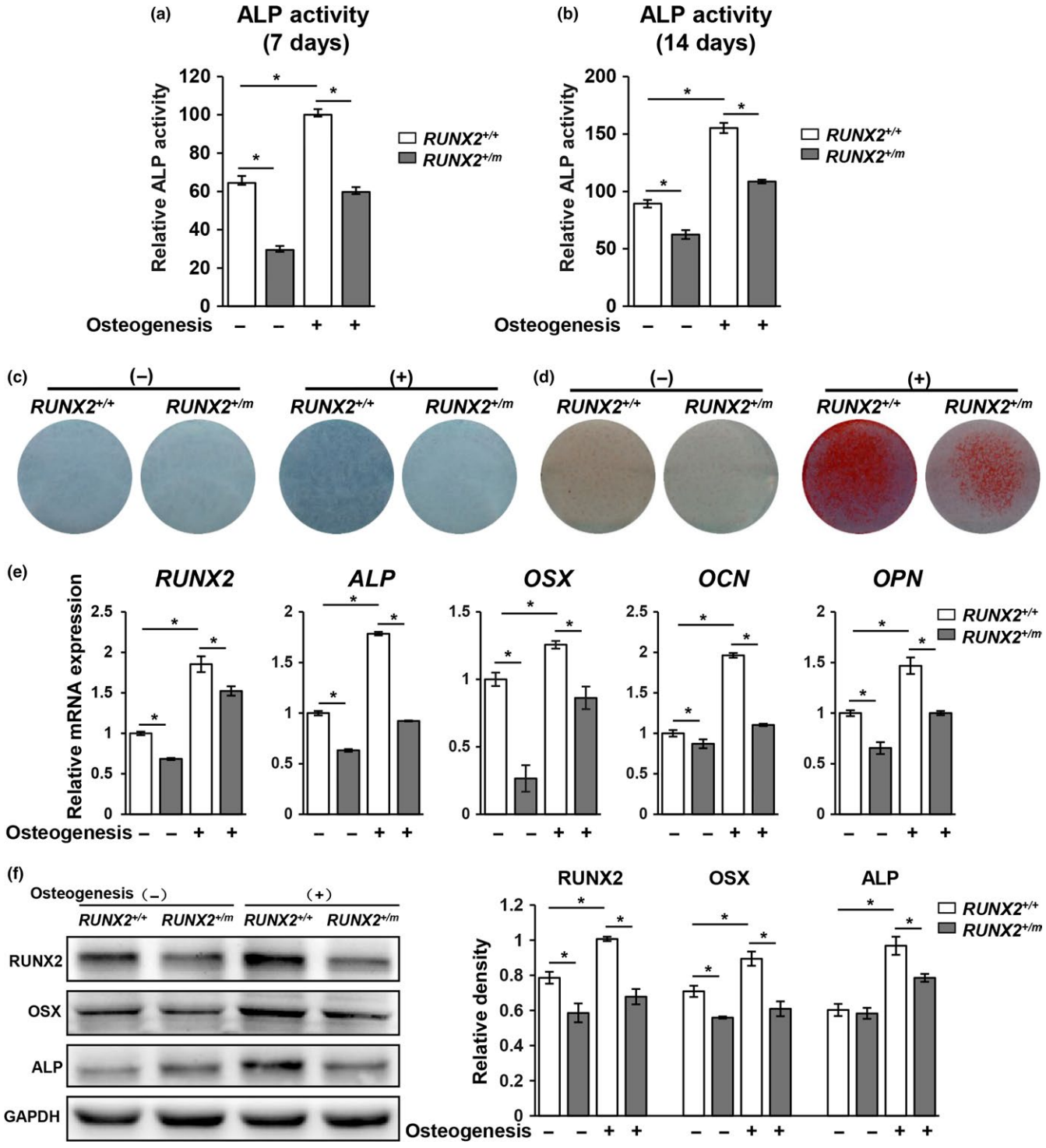

FIGURE 3 DFCs$^{RUNX2+/m}$ exhibited weaker osteogenic potential than DFCs$^{RUNX2+/+}$. Primary DFCs from normal controls (DFCs$^{RUNX2+/+}$) and the cleidocranial dysplasia patient (DFCs$^{RUNX2+/m}$) were cultured in osteogenic induction medium (OIM) for osteogenic differentiation. (a,b) ALP activity of DFCs was analysed after incubation in OIM for 7 days (a) or 14 days (b). (c) ALP staining of DFCs after induction in OIM for 14 days. (d) Alizarin red staining of mineralised nodules for DFCs after induction in OIM for 21 days. (e) Quantitative analysis of the mRNA level of *RUNX2*, *ALP*, *OSX*, *OCN* and *OPN* in DFCs after the cells were treated in OIM for14 days. (f) Western blotting and quantification of RUNX2, ALP and OSX expression in DFCs after the cells were treated in OIM for 14 days. *$p < 0.05$ [Colour figure can be viewed at wileyonlinelibrary.com]

osteogenic induction or not ($p < 0.05$) (Figure 3e). The protein level of RUNX2 in DFCs$^{RUNX2+/m}$ was decreased 30% compared with the normal control ($p < 0.05$) (Figure 3f). In addition, the protein level of OSX and ALP showed a similar pattern with that of RUNX2, which exhibited a 40% reduction in DFCs$^{RUNX2+/m}$ after osteogenic induction ($p < 0.05$) (Figure 3f).

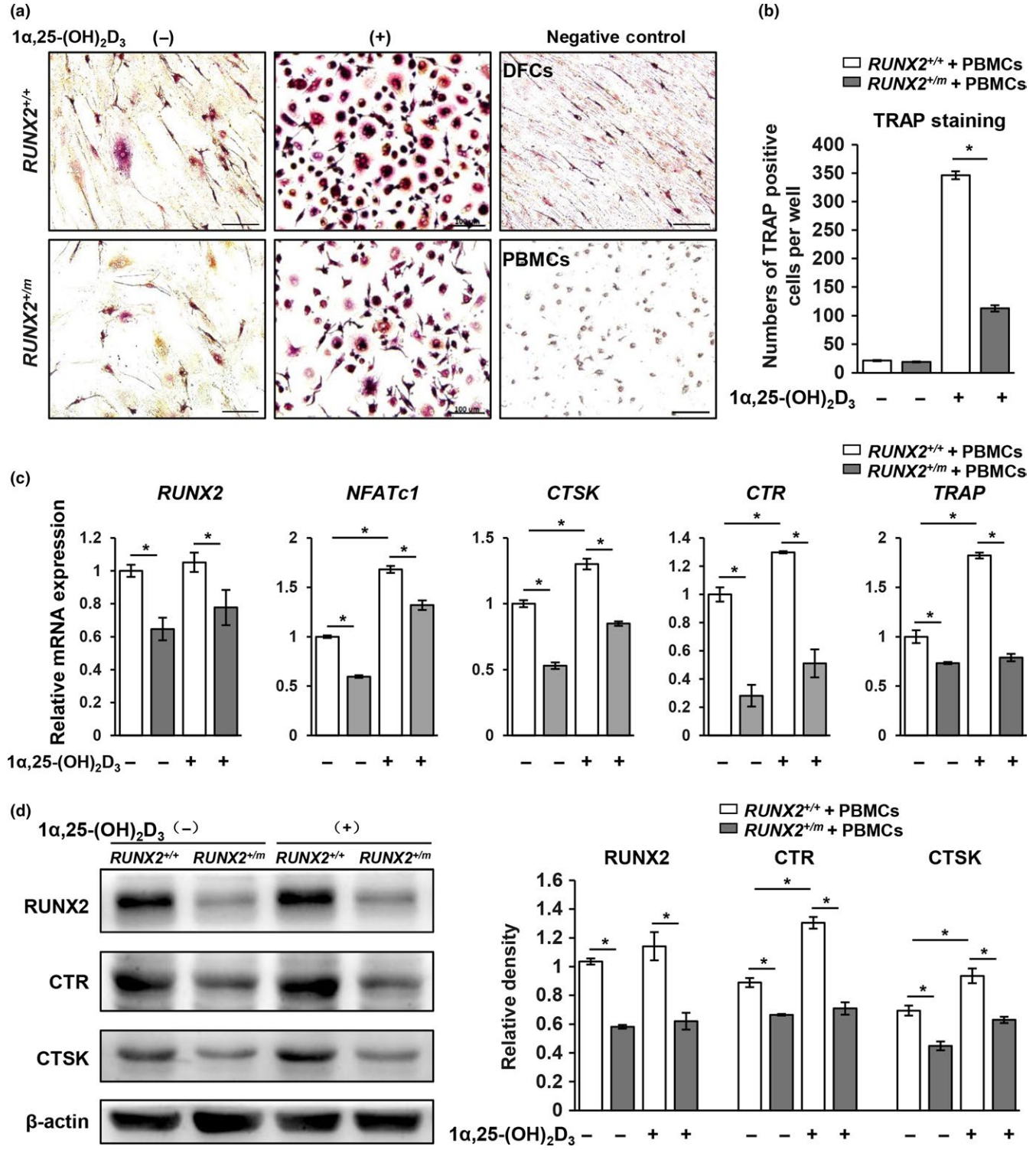

FIGURE 4 DFCs$^{RUNX2+/m}$ exhibited reduced osteoclast-inductive capacity. Primary DFCs from normal control (DFCs$^{RUNX2+/+}$) and the cleidocranial dysplasia patient (DFCs$^{RUNX2+/m}$) were co-cultured with PBMCs for osteoclasts differentiation. (a) TRAP staining of the co-culture of DFCs and PBMCs. Scale bar, 100 μm. (b) The quantification of TRAP$^+$ multinuclear cells in the co-cultures on day 14. (c) Quantitative analysis of the mRNA level of *RUNX2*, *NFATc1*, *CTSK*, *CTR* and *TRAP* in DFCs and PBMCs co-culture. (d) Western blotting and quantification of RUNX2, CTR and CTSK expression in the co-culture of DFCs and PBMCs. *$p < 0.05$ [Colour figure can be viewed at wileyonlinelibrary.com]

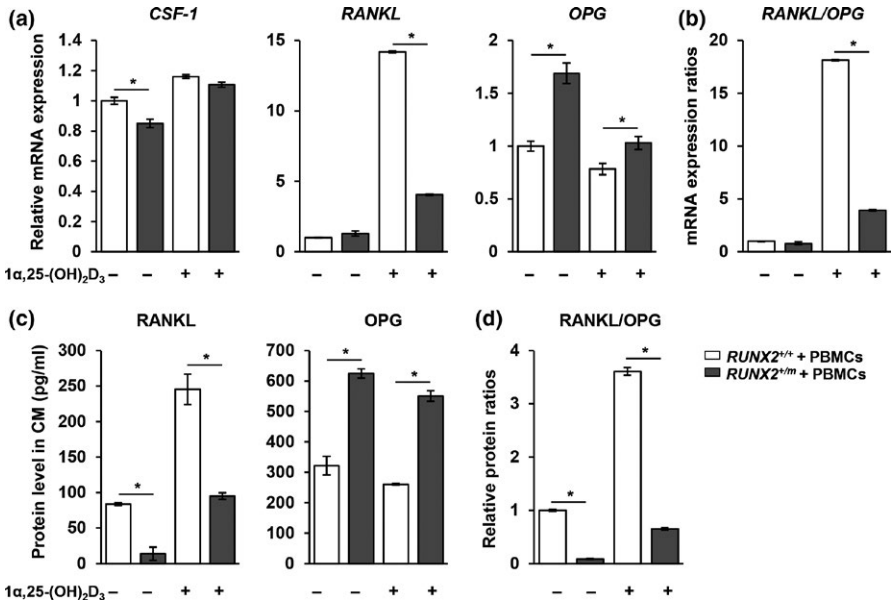

FIGURE 5 DFCs$^{RUNX2+/m}$ restrict osteoclastogenesis through RANKL/RANK/OPG signaling pathway. DFCs were co-cultured with PBMCs for 3 days in the medium containing 1α,25-$(OH)_2D_3$ or an equal volume of vehicle (ethanol). (a) Quantitative analysis of the mRNA level of *CSF-1*, *RANKL* and *OPG* in DFCs and PBMCs co-culture. (b) The ratio of *RANKL/OPG* at mRNA level for DFCs and PBMCs co-culture. (c) The protein level of RANKL and OPG in conditioned medium (CM) collected from the DFCs and PBMC co-culture were analysed by ELISA. (d) The ratio of RANKL/OPG at protein level in CM collected from DFCs and PBMCs co-culture. *$p < 0.05$

3.4 | DFCs$^{RUNX2+/m}$ exhibited reduced osteoclast-inductive capacity

DFCs are able to secrete RNAKL and CSF-1 to induce osteoclast precursors such as PBMCs to differentiate into osteoclasts (Liu et al., 2005; Wise & King, 2008; Yao et al., 2004). To assess the osteoclast-inductive capacity of DFCs$^{RUNX2+/m}$, we performed a co-culture system composed of DFCs and PBMCs. TRAP staining was first carried out to evaluate osteoclastogenesis in the co-culture. Under basal conditions, few TRAP$^+$ cells were present in both DFCs$^{RUNX2+/m}$ and DFCs$^{RUNX2+/+}$ group (Figure 4a,b). Upon 1α,25-$(OH)_2D_3$ stimulation, the number of TRAP$^+$ multinuclear cells in DFCs$^{RUNX2+/m}$ was significantly less than the normal control group ($p < 0.05$) (Figure 4a,b), indicating impaired osteoclast-inductive ability of DFCs$^{RUNX2+/m}$.

The effect of DFCs$^{RUNX2+/m}$ on the expression of osteoclast-associated genes in the co-culture was thereafter explored. Consistent with the abovementioned result, the *RUNX2* mRNA level in the co-culture system of DFCs$^{RUNX2+/m}$ showed a 36% reduction compared with the DFCs$^{RUNX2+/+}$ group ($p < 0.05$) (Figure 4c). The mRNA level of osteoclast-associated genes was also down-regulated in DFCs$^{RUNX2+/m}$ group at different degrees, including nuclear factor of activated T-cells 1 (*NFATc1*), cathepsin K (*CTSK*), calcitonin receptor (*CTR*) and *TRAP* ($p < 0.05$) (Figure 4c). The inhibitory effect of DFCs$^{RUNX2+/m}$ on the expression of osteoclast-associated genes was much clearer upon 1α,25-$(OH)_2D_3$ stimulation ($p < 0.05$) (Figure 4c). Western blot results showed that the RUNX2 protein level was decreased more than 40% in DFCs$^{RUNX2+/m}$ group whether under 1α,25-$(OH)_2D_3$ stimulation or not ($p < 0.05$) (Figure 4d), which was in agreement with the mRNA measurements. Moreover, the protein level of CTR and CTSK in the normal control was up-regulated about 1.5-fold after 1α,25-$(OH)_2D_3$ stimulation, which was inhibited by DFCs$^{RUNX2+/m}$ ($p < 0.05$) (Figure 4d).

3.5 | DFCs$^{RUNX2+/m}$ restricted osteoclastogenesis through RANK/RANKL/OPG signalling pathway

CSF-1 and RANK/RANKL/OPG pathway play important roles in the process of osteoclasts differentiation (Nakashima, Hayashi, & Takayanagi, 2012; Que & Wise, 1997). To investigate the mechanism of the reduced osteoclast-inductive capacity of DFCs$^{RUNX2+/m}$, the expression of CSF-1, RANKL, and OPG in the co-culture of DFCs and PBMCs was detected. The basal mRNA level of *CSF-1* in the DFCs$^{RUNX2+/m}$ group was slightly lower than the normal control ($p < 0.05$), while this difference between the two groups disappeared upon 1α,25-$(OH)_2D_3$ stimulation (Figure 5a). Strikingly, the mRNA level of *RANKL* in the DFCs$^{RUNX2+/+}$ group increased 14-fold after 1α,25-$(OH)_2D_3$ stimulation ($p < 0.05$), while this increase was almost blocked by DFCs$^{RUNX2+/m}$ (Figure 5a). In contrast, *OPG* expression was reduced after 1α,25-$(OH)_2D_3$ stimulation, and the mRNA level of *OPG* in the DFCs$^{RUNX2+/m}$ group was up-regulated more than 1.3-fold compared with the normal control ($p < 0.05$) (Figure 5a). Accordingly, the ratio of *RANKL/OPG* was increased 18-fold in the normal control upon 1α,25-$(OH)_2D_3$ stimulation, and this increase was blocked by DFCs$^{RUNX2+/m}$ ($p < 0.05$) (Figure 5b).

The protein level of RANKL and OPG in the conditioned medium of the co-culture system was thereafter investigated.

Consistent with the mRNA measurements, RANKL protein concentration in the normal control showed a 2.5-fold increase after 1α,25-$(OH)_2D_3$ stimulation ($p < 0.05$), while OPG expression was unaffected by 1α,25-$(OH)_2D_3$ stimulation (Figure 5c). RANKL protein concentration in the DFCs$^{RUNX2+/m}$ group was decreased 60%, and OPG was increased 2-fold compared with the normal control both in basal and 1α,25-$(OH)_2D_3$ stimulated conditions ($p < 0.05$) (Figure 5c). Consequently, the ratio of RANKL/OPG was reduced 80% by DFCs$^{RUNX2+/m}$ ($p < 0.05$) (Figure 5d). All these results indicated that the RANK/RANKL/OPG signalling pathway was impaired by DFCs$^{RUNX2+/m}$.

4 | DISCUSSION

In this study, we found that the novel *RUNX2* missense mutation (c. 557G>C, p. R186T) down-regulated the expression of osteogenesis-related genes, leading to a decrease in osteogenic capacity of DFCs$^{RUNX2+/m}$. In addition, DFCs$^{RUNX2+/m}$ reduced osteoclasts differentiation and the expression of osteoclast-related genes, including *NFATc1*, *CTSK*, *CTR* and *TRAP*. Our further study confirmed that the decreased osteoclast-inductive ability of DFCs$^{RUNX2+/m}$ was mediated by RANK/RANKL/OPG signalling pathway. These findings preliminarily revealed the mechanism of delayed tooth eruption in CCD patients.

RUNX2 has several function domains, including a glutamine-alanine repeat (Q/A) domain, a highly conserved Runt domain, a nuclear localisation signal (NLS) and a proline-serine-threonine rich (PST) domain from the N-terminal to the C-terminal (Bruderer et al., 2014). The *RUNX2* mutation (c. 557G>C, p. R186T) found in the present CCD patient is located in the Runt domain, which encodes the evolutionarily conserved protein structure that defines the RUNXs family (Tahirov et al., 2001). The Runt domain is mainly responsible for DNA binding to a specific motif and heterodimerization with core binding factor β (CBFβ) (Tahirov et al., 2001). Thus, the missense mutation resulting in a conversion of arginine 186 could potentially affect the biological function of RUNX2. However, our research group has confirmed that p.R186T RUNX2 showed normal nuclear localisation and decreased transactivation capacity (Zhang et al., 2017). Furthermore, previous studies showed that conversion of arginine 135 in Runt domain, which corresponds to arginine 186 of RUNX2, abrogates DNA binding ability of Runt domain but does not perturb heterodimerization with CBFβ (Nagata & Werner, 2001; Preudhomme et al., 2000). In addition, many other studies also reported that some mutant RUNX2, which contains missense mutations in Runt domain, is capable of heterodimerizing with CBFβ, but cannot bind the RUNX2 recognition motif (Han et al., 2010; Yoshida et al., 2002). Collectively, current evidence suggests that p.R186T RUNX2 may lose DNA binding capacity but retain heterodimerization with CBFβ. However, it still remains to be verified by further experiments in the future.

It has been reported that RUNX2 is involved in controlling cell proliferation and regulating the cell cycle-related genes (Ruffenach et al., 2016). However, the proliferation rate of DFCs$^{RUNX2+/m}$ showed no difference compared with DFCs$^{RUNX2+/+}$ in the present study. Previous studies by other researchers reported that *RUNX2* mutation showed conflicting role on cell proliferation (Ge et al., 2015; Li et al., 2014; Sun et al., 2016; Wang et al., 2016; Yan et al., 2015). We speculated that different cell type and environment among studies might be responsible for the inconsistent results. Further investigations are yet needed to explore the mechanism of *RUNX2* mutation on cell proliferation.

Tooth eruption is a localised event that requires bone resorption and bone formation in the given tooth crypt (Wise et al., 2007). It is reported that bone formation at the base of tooth crypt serves as a motive force to propel the tooth out of its bony crypt (Wise et al., 2007, 2011). The present study showed that the ALP activity and the ability to form mineralised nodules of DFCs$^{RUNX2+/m}$ was disturbed. These results were somewhat predictable because of the crucial role of RUNX2 in osteoblasts differentiation and bone formation. As a critical osteogenesis-specific transcription factor, RUNX2 was found to be constitutively expressed in differentiated DFCs (Morsczeck et al., 2009). RUNX2 over-expression could up-regulate the expression of osteoblast-related genes and in vitro enhance osteogenic differentiation of DFCs (Pan et al., 2010). In the current study, we found that the stimulating function of RUNX2 on the osteogenic differentiation was inhibited by DFCs$^{RUNX2+/m}$, which was further confirmed by the inhibitory effect of DFCs$^{RUNX2+/m}$ on the expression of osteogenic-related genes, including *RUNX2*, *ALP*, *OSX*, *OCN* and *OPN*. These findings were also consistent with our recent report on dental pulp cells (DPCs) (Yan et al., 2015).

During tooth eruption, osteoclastogenesis in the coronal area of tooth bulb is crucial for bone resorption and the formation of tooth eruption pathway (Wise & King, 2008). DFCs are critical for tooth eruption by secreting some important factors that are essential for osteoclastogenesis. It is well known that at the early stage of osteoclastogenesis, DFCs secrete CSF-1 and MCP-1 to the dental follicles in order to promote the recruitment of osteoclast precursors, and then RANKL is secreted by DFCs and binds to RANK to promote the development of osteoclasts (Nakashima & Takayanagi, 2009; Nakashima et al., 2012; Que & Wise, 1997). In addition, the high level of CSF-1 can also reduce the expression of OPG and secreted frizzled-related protein-1 (SFRP1), which are inhibitors of osteoclasts differentiation (Liu & Wise, 2007; Wise & King, 2008). However, the molecular process occurred in the dental follicles, which is critical for tooth eruption to regulate the burst of osteoclastogenesis, remains unclear in CCD patients who are usually common with *RUNX2* heterozygous mutation or deletion. In the present study, we find that osteoclasts differentiation and the expression of osteoclast-associated markers, including *NFATc1*, *CTSK*, *CTR* and *TRAP*, are severely disturbed by DFCs$^{RUNX2+/m}$. These results indicate that DFCs$^{RUNX2+/m}$ can impair osteoclastogenesis in the local region during tooth eruption. Other studies had also reported that *RUNX2* mutation could markedly restrict the ability of DFCs and PDLCs to induce osteoclasts differentiation, which was consistent with the results in the current study (Dorotheou et al., 2013; Ge et al., 2015; Lossdorfer et al., 2009).

Osteoclasts differentiate from hematopoietic precursor cells through direct contact with osteoblastic/stromal cells (Boyle, Simonet,

& Lacey, 2003). RANK/RANKL/OPG pathway plays an essential role in the regulation of osteoclastogenesis (Han et al., 2001; Zhang, Heulsmann, Tondravi, Mukherjee, & Abu-Amer, 2001). RANKL binds to its receptor RANK in the osteoclast-precursor cells and activates several key molecules to stimulate maturation of osteoclasts (Ouyang et al., 2014). OPG, which binds RANKL with higher affinity than RANK, acts as a decoy receptor for RANKL and inhibits osteoclasts differentiation and activation (Takahashi, Maeda, Ishihara, Uehara, & Kobayashi, 2011). In addition, CSF-1, which is secreted by osteoblastic/stromal cells, is also required for osteoclasts differentiation and activation (Novack, 2011). In the present study, we found that DFCs$^{RUNX2+/m}$ reduced the expression of RANKL and CSF-1 while increased the expression of OPG, thereafter down-regulated the ratio of RANKL/OPG, which could reflect the potentiality of osteoclasts differentiation in the local region. Our explanation is that RUNX2 binding elements are present in the promoter region of RANKL and OPG (Byon et al., 2011; Thirunavukkarasu et al., 2001). RUNX2 can induce RANKL expression and suppress OPG expression in vitro, leading to the promotion of osteoclasts differentiation (Byon et al., 2011; Enomoto et al., 2003). Studies also showed that overexpression of RANKL could partially rescue the blockage of osteoclasts differentiation in RUNX2 deficient mice, indicating that RUNX2 was involved in osteoclastogenesis by regulating RANK/RANKL/OPG signalling (Enomoto et al., 2003). Therefore, the disturbed RANK/RANKL/OPG pathway owing to DFCs$^{RUNX2+/m}$ may be the reason for the impaired bone resorption, which would restrict the formation of eruption pathway and thereafter result in delayed tooth eruption in CCD patients.

In summary, our findings indicate that DFCs$^{RUNX2+/m}$ exhibits down-regulated expression of osteoblast-specific genes, leading to reduced osteogenic capacity, therefore interferes with the bone formation at the base of tooth crypt, which serves as a motive force for tooth eruption. In addition, DFCs$^{RUNX2+/m}$ disturbs osteoclasts differentiation through RANK/RANKL/OPG signalling pathway, down-regulates the expression of osteoclast-related genes in osteoclast-precursor cells, and consequently restricts the function of osteoclastogenesis and the formation of tooth eruption pathway. These two aspects work in coordination causing the delayed permanent tooth eruption in CCD patients. Our study systematically reveals the mechanism for the delayed permanent tooth eruption owing to *RUNX2* mutation in CCD patients.

ACKNOWLEDGEMENTS

This work was supported by the National Natural Science Foundation of China (grant number 81771053) and Peking University School and Hospital of Stomatology Science Foundation for Young Scientists (grant number PKUSS20160105). The authors are very grateful to all the participants in this study.

CONFLICT OF INTERESTS

None to declare.

AUTHOR CONTRIBUTION

Yang Liu contributed to conception, design, data analysis, drafted and critically revised the manuscript; Xianli Zhang contributed to data acquisition and interpretation; Xiangyu Sun contributed to data analysis and drafting the manuscript; Xiaozhe Wang contributed to data acquisition and critically revised the manuscript; Chenying Zhang contributed to data acquisition and analysis, drafting and critical revision of the manuscript. Shuguo Zheng contributed to design, data analysis, and critically revised the manuscript.

ORCID

Yang Liu http://orcid.org/0000-0003-2359-6583
Shuguo Zheng http://orcid.org/0000-0001-6717-5196

REFERENCES

Boyle, W. J., Simonet, W. S., & Lacey, D. L. (2003). Osteoclast differentiation and activation. *Nature*, *423*, 337–342. https://doi.org/10.1038/nature01658

Bruderer, M., Richards, R. G., Alini, M., & Stoddart, M. J. (2014). Role and regulation of RUNX2 in osteogenesis. *European Cells & Materials*, *28*, 269–286. https://doi.org/10.22203/eCM

Byon, C. H., Sun, Y., Chen, J., Yuan, K., Mao, X., Heath, J. M., … Chen, Y. (2011). Runx2-upregulated receptor activator of nuclear factor kappaB ligand in calcifying smooth muscle cells promotes migration and osteoclastic differentiation of macrophages. *Arteriosclerosis, thrombosis, and vascular biology*, *31*, 1387–1396. https://doi.org/10.1161/ATVBAHA.110.222547

Camilleri, S., & McDonald, F. (2006). Runx2 and dental development. *European journal of oral sciences*, *114*, 361–373. https://doi.org/10.1111/j.1600-0722.2006.00399.x

Chen, P., Wei, D., Xie, B., Ni, J., Xuan, D., & Zhang, J. (2014). Effect and possible mechanism of network between microRNAs and RUNX2 gene on human dental follicle cells. *Journal of cellular biochemistry*, *115*, 340–348. https://doi.org/10.1002/jcb.24668

Dorotheou, D., Gkantidis, N., Karamolegkou, M., Kalyvas, D., Kiliaridis, S., & Kitraki, E. (2013). Tooth eruption: Altered gene expression in the dental follicle of patients with cleidocranial dysplasia. *Orthodontics & craniofacial research*, *16*, 20–27. https://doi.org/10.1111/ocr.12000

Enomoto, H., Shiojiri, S., Hoshi, K., Furuichi, T., Fukuyama, R., Yoshida, C. A., … Komori, T. (2003). Induction of osteoclast differentiation by Runx2 through receptor activator of nuclear factor-kappa B ligand (RANKL) and osteoprotegerin regulation and partial rescue of osteoclastogenesis in Runx2-/- mice by RANKL transgene. *The Journal of Biological Chemistry*, *278*, 23971–23977. https://doi.org/10.1074/jbc.M302457200

Ge, J., Guo, S., Fu, Y., Zhou, P., Zhang, P., Du, Y., … Jiang, H. (2015). Dental follicle cells participate in tooth eruption via the RUNX2-MiR-31-SATB2 loop. *Journal of dental research*, *94*, 936–944. https://doi.org/10.1177/0022034515578908

Han, J. H., Choi, S. J., Kurihara, N., Koide, M., Oba, Y., & Roodman, G. D. (2001). Macrophage inflammatory protein-1alpha is an osteoclastogenic factor in myeloma that is independent of receptor activator of nuclear factor kappaB ligand. *Blood*, *97*, 3349–3353. https://doi.org/10.1182/blood.V97.11.3349

Han, M. S., Kim, H. J., Wee, H. J., Lim, K. E., Park, N. R., Bae, S. C., … Choi, J. Y. (2010). The cleidocranial dysplasia-related R131G mutation in the Runt-related transcription factor RUNX2 disrupts binding to DNA but not CBF-beta. *Journal of cellular biochemistry*, *110*, 97–103.

Jensen, B. L., & Kreiborg, S. (1990). Development of the dentition in cleidocranial dysplasia. *Journal of oral pathology & medicine*, *19*, 89–93. https://doi.org/10.1111/j.1600-0714.1990.tb00803.x

Li, B., Zhang, Y., Wang, Q., Dong, Z., Shang, L., Wu, L., … Jin, Y. (2014). Periodontal ligament stem cells modulate root resorption of human primary teeth via Runx2 regulating RANKL/OPG system. *Stem cells and development*, *23*, 2524–2534. https://doi.org/10.1089/scd.2014.0127

Liu, D., & Wise, G. E. (2007). A DNA microarray analysis of chemokine and receptor genes in the rat dental follicle–role of secreted frizzled-related protein-1 in osteoclastogenesis. *Bone*, *41*, 266–272. https://doi.org/10.1016/j.bone.2007.04.181

Liu, D., Yao, S., Pan, F., & Wise, G. E. (2005). Chronology and regulation of gene expression of RANKL in the rat dental follicle. *European journal of oral sciences*, *113*, 404–409. https://doi.org/10.1111/j.1600-0722.2005.00245.x

Lossdorfer, S., Abou Jamra, B., Rath-Deschner, B., Gotz, W., Abou Jamra, R., Braumann, B., & Jager, A. (2009). The role of periodontal ligament cells in delayed tooth eruption in patients with cleidocranial dysostosis. *Journal of Orofacial Orthopedics*, *70*, 495–510. https://doi.org/10.1007/s00056-009-9934-x

Morsczeck, C., Schmalz, G., Reichert, T. E., Vollner, F., Saugspier, M., Viale-Bouroncle, S., & Driemel, O. (2009). Gene expression profiles of dental follicle cells before and after osteogenic differentiation in vitro. *Clinical oral investigations*, *13*, 383–391. https://doi.org/10.1007/s00784-009-0260-x

Mundlos, S. (1999). Cleidocranial dysplasia: Clinical and molecular genetics. *Journal of medical genetics*, *36*, 177–182.

Mundlos, S., Otto, F., Mundlos, C., Mulliken, J. B., Aylsworth, A. S., Albright, S., … Olsen, B. R. (1997). Mutations involving the transcription factor CBFA1 cause cleidocranial dysplasia. *Cell*, *89*, 773–779. https://doi.org/10.1016/S0092-8674(00)80260-3

Nagata, T., & Werner, M. H. (2001). Functional mutagenesis of AML1/RUNX1 and PEBP2 beta/CBF beta define distinct, non-overlapping sites for DNA recognition and heterodimerization by the Runt domain. *Journal of molecular biology*, *308*, 191–203. https://doi.org/10.1006/jmbi.2001.4596

Nakashima, T., Hayashi, M., & Takayanagi, H. (2012). New insights into osteoclastogenic signaling mechanisms. *Trends in Endocrinology and Metabolism: TEM*, *23*, 582–590. https://doi.org/10.1016/j.tem.2012.05.005

Nakashima, T., & Takayanagi, H. (2009). Osteoimmunology: Crosstalk between the immune and bone systems. *Journal of clinical immunology*, *29*, 555–567. https://doi.org/10.1007/s10875-009-9316-6

Novack, D. V. (2011). Role of NF-kappaB in the skeleton. *Cell research*, *21*, 169–182. https://doi.org/10.1038/cr.2010.159

Ouyang, Z., Zhai, Z., Li, H., Liu, X., Qu, X., Li, X., … Dai, K. (2014). Hypericin suppresses osteoclast formation and wear particle-induced osteolysis via modulating ERK signalling pathway. *Biochemical pharmacology*, *90*, 276–287. https://doi.org/10.1016/j.bcp.2014.06.009

Pan, K., Sun, Q., Zhang, J., Ge, S., Li, S., Zhao, Y., & Yang, P. (2010). Multilineage differentiation of dental follicle cells and the roles of Runx2 over-expression in enhancing osteoblast/cementoblast-related gene expression in dental follicle cells. *Cell proliferation*, *43*, 219–228. https://doi.org/10.1111/j.1365-2184.2010.00670.x

Preudhomme, C., Warot-Loze, D., Roumier, C., Grardel-Duflos, N., Garand, R., Lai, J. L., … Fenaux, P. (2000). High incidence of biallelic point mutations in the Runt domain of the AML1/PEBP2 alpha B gene in Mo acute myeloid leukemia and in myeloid malignancies with acquired trisomy 21. *Blood*, *96*, 2862–2869.

Quack, I., Vonderstrass, B., Stock, M., Aylsworth, A. S., Becker, A., Brueton, L., … Otto, F. (1999). Mutation analysis of core binding factor A1 in patients with cleidocranial dysplasia. *American journal of human genetics*, *65*, 1268–1278. https://doi.org/10.1086/302622

Que, B. G., & Wise, G. E. (1997). Colony-stimulating factor-1 and monocyte chemotactic protein-1 chemotaxis for monocytes in the rat dental follicle. *Archives of oral biology*, *42*, 855–860. https://doi.org/10.1016/S0003-9969(97)00072-1

Ruffenach, G., Chabot, S., Tanguay, V. F., Courboulin, A., Boucherat, O., Potus, F., … Bonnet, S. (2016). Role for runt-related transcription factor 2 in proliferative and calcified vascular lesions in pulmonary arterial hypertension. *American journal of respiratory and critical care medicine*, *194*, 1273–1285. https://doi.org/10.1164/rccm.201512-2380OC

Saugspier, M., Felthaus, O., Viale-Bouroncle, S., Driemel, O., Reichert, T. E., Schmalz, G., & Morsczeck, C. (2010). The differentiation and gene expression profile of human dental follicle cells. *Stem cells and development*, *19*, 707–717. https://doi.org/10.1089/scd.2010.0027

Sun, X., Wang, X., Zhang, C., Liu, Y., Yang, X., Yan, W., … Zheng, S. (2016). RUNX2 mutation impairs bone remodelling of dental follicle cells and periodontal ligament cells in patients with cleidocranial dysplasia. *Mutagenesis*, *31*, 677–685. https://doi.org/10.1093/mutage/gew039

Tahirov, T. H., Inoue-Bungo, T., Morii, H., Fujikawa, A., Sasaki, M., Kimura, K., … Ogata, K. (2001). Structural analyses of DNA recognition by the AML1/Runx-1 Runt domain and its allosteric control by CBFbeta. *Cell*, *104*, 755–767. https://doi.org/10.1016/S0092-8674(01)00271-9

Takahashi, N., Maeda, K., Ishihara, A., Uehara, S., & Kobayashi, Y. (2011). Regulatory mechanism of osteoclastogenesis by RANKL and Wnt signals. *Frontiers in Bioscience (Landmark edition)*, *16*, 21–30. https://doi.org/10.2741/3673

Thirunavukkarasu, K., Miles, R. R., Halladay, D. L., Yang, X., Galvin, R. J., Chandrasekhar, S., … Onyia, J. E. (2001). Stimulation of osteoprotegerin (OPG) gene expression by transforming growth factor-beta (TGF-beta). Mapping of the OPG promoter region that mediates TGF-beta effects. *The Journal of Biological Chemistry*, *276*, 36241–36250. https://doi.org/10.1074/jbc.M104319200

Wang, X. Z., Sun, X. Y., Zhang, C. Y., Yang, X., Yan, W. J., Ge, L. H., & Zheng, S. G. (2016). RUNX2 mutation impairs 1alpha,25-Dihydroxyvitamin D3 mediated osteoclastogenesis in dental follicle cells. *Scientific reports*, *6*, 24225. https://doi.org/10.1038/srep24225

Wise, G. E. (2009). Cellular and molecular basis of tooth eruption. *Orthodontics & craniofacial research*, *12*, 67–73. https://doi.org/10.1111/j.1601-6343.2009.01439.x

Wise, G. E., He, H., Gutierrez, D. L., Ring, S., & Yao, S. (2011). Requirement of alveolar bone formation for eruption of rat molars. *European journal of oral sciences*, *119*, 333–338. https://doi.org/10.1111/j.1600-0722.2011.00854.x

Wise, G. E., & King, G. J. (2008). Mechanisms of tooth eruption and orthodontic tooth movement. *Journal of dental research*, *87*, 414–434. https://doi.org/10.1177/154405910808700509

Wise, G. E., Yao, S., & Henk, W. G. (2007). Bone formation as a potential motive force of tooth eruption in the rat molar. *Clinical anatomy*, *20*, 632–639. https://doi.org/10.1002/(ISSN)1098-2353

Yan, W. J., Zhang, C. Y., Yang, X., Liu, Z. N., Wang, X. Z., Sun, X. Y., … Zheng, S. G. (2015). Abnormal differentiation of dental pulp cells in cleidocranial dysplasia. *Journal of dental research*, *94*, 577–583. https://doi.org/10.1177/0022034514566655

Yao, S., Ring, S., Henk, W. G., & Wise, G. E. (2004). In vivo expression of RANKL in the rat dental follicle as determined by laser capture microdissection. *Archives of oral biology*, *49*, 451–456. https://doi.org/10.1016/j.archoralbio.2004.01.009

Yoda, S., Suda, N., Kitahara, Y., Komori, T., & Ohyama, K. (2004). Delayed tooth eruption and suppressed osteoclast number in the eruption pathway of heterozygous Runx2/Cbfa1 knockout mice. *Archives of oral biology*, *49*, 435–442. https://doi.org/10.1016/j.archoralbio.2004.01.010

Yoshida, T., Kanegane, H., Osato, M., Yanagida, M., Miyawaki, T., Ito, Y., & Shigesada, K. (2002). Functional analysis of RUNX2 mutations in Japanese patients with cleidocranial dysplasia demonstrates novel genotype-phenotype correlations. *American journal of human genetics*, *71*, 724–738. https://doi.org/10.1086/342717

Zhang, Y. H., Heulsmann, A., Tondravi, M. M., Mukherjee, A., & Abu-Amer, Y. (2001). Tumor necrosis factor-alpha (TNF) stimulates RANKL-induced osteoclastogenesis via coupling of TNF type 1 receptor and RANK signaling pathways. *The Journal of Biological Chemistry*, *276*, 563–568. https://doi.org/10.1074/jbc.M008198200

Zhang, X., Liu, Y., Wang, X., Sun, X., Zhang, C., & Zheng, S. (2017). Analysis of novel RUNX2 mutations in Chinese patients with cleidocranial dysplasia. *PLoS ONE*, *12*, e0181653. https://doi.org/10.1371/journal.pone.0181653

Zhang, H., Wang, J., Deng, F., Huang, E., Yan, Z., Wang, Z., … Deng, F. (2015). Canonical Wnt signaling acts synergistically on BMP9-induced osteo/odontoblastic differentiation of stem cells of dental apical papilla (SCAPs). *Biomaterials*, *39*, 145–154. https://doi.org/10.1016/j.biomaterials.2014.11.007

How to cite this article: Liu Y, Zhang X, Sun X, Wang X, Zhang C, Zheng S. Abnormal bone remodelling activity of dental follicle cells from a cleidocranial dysplasia patient. *Oral Dis*. 2018;24:1270–1281. https://doi.org/10.1111/odi.12900